The Astrophysical Journal, 810:20 (8pp), 2015 September 1 doi:10.1088/0004-637X/810/1/20

NATURE OF THE EXTREME ULTRALUMINOUS X-RAY SOURCES

Grzegorz Wiktorowicz[1], Małgorzata Sobolewska[2], Aleksander Sądowski[3], and Krzysztof Belczynski[1,4]
[1] Astronomical Observatory, University of Warsaw, Al. Ujazdowskie 4, 00-478 Warsaw, Poland; gwiktoro@astrouw.edu.pl
[2] Nicolaus Copernicus Astronomical Center, Bartycka 18, 00-716 Warsaw, Poland
[3] MIT Kavli Institute for Astrophysics and Space Research 77 Massachusetts Ave, Cambridge, MA 02139, USA
Received 2015 March 31; accepted 2015 July 21; published 2015 August 25

ABSTRACT

In this proof-of-concept study we demonstrate that in a binary system mass can be transferred toward an accreting compact object at an extremely high rate. If the transferred mass is efficiently converted to X-ray luminosity (with disregard of the classical Eddington limit) or if the X-rays are focused into a narrow beam, then binaries can form extreme ultraluminous X-ray (ULX) sources with an X-ray luminosity of $L_{\rm X} \gtrsim 10^{42}$ erg s^{-1}. For example, Lasota and King argued that the brightest known ULX (HLX-1) is a regular binary system with a rather low-mass compact object (a stellar-origin black hole (BH) or a neutron star (NS)). The predicted formation efficiencies and lifetimes of binaries with the very high mass transfer rates are large enough to explain *all* observed systems with extreme X-ray luminosities. These systems are not only limited to binaries with stellar-origin BH accretors. Notably, we have also identified such objects with NSs. Typically, a 10 $M_{\odot}$ BH is fed by a massive ($\sim$10 $M_{\odot}$) Hertzsprung gap donor with Roche lobe overflow (RLOF) rate of $\sim 10^{-3}\ M_{\odot}$ yr^{-1} ($\approx 2600 \dot{M}_{\rm Edd}$). For NS systems the typical donors are evolved low-mass ($\sim$2 $M_{\odot}$) helium stars with RLOF rate of $\sim 10^{-2}\ M_{\odot}$ yr^{-1}. Our study does not prove that any particular extreme ULX is a regular binary system, but it demonstrates that *any* ULX, including the most luminous ones, may potentially be a short-lived phase in the life of a binary star.

Key words: stars: black holes – stars: neutron – X-rays: binaries

1. INTRODUCTION

Our universe is populated with black holes (BHs) and neutron stars (NSs) in various binary configurations. In our Galaxy, many such binaries show significant X-ray activity suggestive of a mass transfer and accretion onto the compact star. X-ray luminosities of only two Galactic X-ray binaries (XRBs) exceed $\sim 10^{39}$ erg s^{-1} (approximately the Eddington limit for a 10 $M_{\odot}$ BH) in GRS 1915 + 105 (Fender & Belloni 2004) and possibly in SS 433 if the system were observed along the jet axis (Fabrika et al. 2006).

However, a large population of extra-galactic point-like X-ray sources with luminosities in excess of $\sim 10^{39}$ erg s^{-1} has been identified (e.g., Fabbiano et al. 1989; Liu 2011; Walton et al. 2011). These so-called ultraluminous X-ray sources (ULX) are off-nuclear and therefore accretion onto a super-massive BH ($M > 10^5\ M_{\odot}$) can be excluded as the source of their luminosity. Instead, the two most popular scenarios to explain their nature include binary systems hosting (i) a stellar mass BH accreting at a super-Eddington rate, or (ii) an intermediate mass BH (IMBH) and sub-Eddington accretion (Colbert & Mushotzky 1999). In the latter case, formation of BHs heavier than $\sim$100 $M_{\odot}$ presents a problem for current models of stellar evolution. Although, it has been suggested that such IMBHs may be formed in dense globular clusters (Miller & Hamilton 2002) or even as a result of stellar evolution of very massive stars ($\sim$200–300 $M_{\odot}$; Crowther et al. 2010; Yusof et al. 2013).

The super-Eddington BH accretion invoked in the stellar origin scenario remains still a relatively poorly understood regime. However, several theoretical mechanisms able to breach the Eddington limit have been proposed, e.g., beaming (e.g., King et al. 2001; Poutanen et al. 2007; King 2008) and/or hyper-accretion allowed by non-uniform escape of photons from accretion flow ("photonic bubbles"; Begelman et al. 2006), as well as a contribution of rotation powered pulsars and pulsar wind nebulae to the ULX population (Medvedev & Poutanen 2013).

Robust observational constraints on the mass of the accretor in some ULXs (e.g., Motch et al. 2014) indicate that indeed super-Eddington accretion onto stellar-origin BHs is realized in nature. Moreover, Bachetti et al. (2014) investigating the M82 X-2 source have demonstrated that the super-Eddington accretion is also possible in XRBs hosting a NS. Additionally, some sources transit relatively fast between the super- and sub-Eddington regimes on timescales as short as a few days to a week (e.g., Bachetti et al. 2013; Walton et al. 2013). Such short timescales are in contradiction with IMBH accretors (Lasota 2015).

Nevertheless, it has been speculated that the brightest ULXs, with luminosities $>10^{41}$ erg s^{-1} may be candidate IMBHs (e.g., Sutton et al. 2012). Recently, compelling evidence, based on quasi-periodic oscillations (QPO), was presented in support of a $\sim$400 $M_{\odot}$ BH in M82 X-1 (Pasham et al. 2014). However, it was also suggested that these QPOs may be harmonics of pulsar rotation periods (Kluźniak & Lasota 2015). Moreover, Sutton et al. (2015) demonstrated that the IMBH candidate in IC 4320 is actually a background active galactic nucleus. To date, HLX-1 with $L_{\rm X} = 1.1 \times 10^{42}$ erg s^{-1} (Farrell et al. 2011) is the brightest known ULX (for a discussion of the brightest ULXs see Servillat et al. 2011).

We approach the ULX issue from the standpoint of one particular evolutionary model for binary evolution. We consider only the far end of the ULX luminosity space, $L_{\rm X} \gtrsim 10^{42}$ erg s^{-1}, and we refer to the sources potentially able to reach these luminosities as extreme ULXs (EULXs). We explore the possibility that EULXs are binary systems with Roche lobe overflow (RLOF) mass transfer rates that highly exceed the classical Eddington limit. For the purpose of this

[4] Warsaw Virgo Group.

proof-of-concept study, we assume that the transferred mass is efficiently accreted onto a compact object and converted to X-ray luminosity in the full range of possible mass accretion rates. This is in contrast with the generally accepted view that the conversion efficiency decreases with increasing mass accretion rate (e.g., Poutanen et al. 2007). However, if mass is lost during accretion process and even if conversion into X-ray luminosity is not fully efficient, a geometrical beaming can provide large X-ray luminosities for sources considered in our study.

2. MODEL

We employ the binary population synthesis code, `StarTrack` (Belczynski et al. 2008a), with updates as discussed in Dominik et al. (2015) with the following initial conditions: a Kroupa et al. (1993) broken power law for initial mass function (IMF; primary mass between 6 and 150 $M_\odot$), flat mass ratio distribution (Kobulnicky et al. 2006; secondary mass between 0.08 and 150 $M_\odot$), flat in logarithm distribution of separations (Abt 1983; $f(a) \sim 1/a$) and thermal distribution of eccentricities (Duquennoy & Mayor 1991 $f(e) \sim e$).

We use the `BOINC` platform[5] for volunteer computing in our program ``universe@home'' (http://universeathome.pl) to obtain a large number of XRBs ($N = 10^9$ of massive binary systems were evolved by volunteers). The X-ray binary is defined as a system hosting a donor star transferring mass via RLOF to a compact object companion (NS or BH). For any given system our evolutionary models provide the donor RLOF mass transfer rate, $\dot{M}_{\rm RLOF}$. The accretion rate onto the compact object, $\dot{M}_{\rm acc}$, is estimated in three different ways from the mass transfer rate (see below).

We search for evolutionary channels that allow for the formation of binaries with highest possible RLOF mass transfer rates onto stellar-origin BHs and NSs. Conservatively, we model only solar metallicity ($Z_\odot = 0.02$; Villante et al. 2014) and we allow IMF to extend only to 150 $M_\odot$. Note that lower metallicity and higher mass stars may form massive ($\gtrsim$100 $M_\odot$) BHs in binary systems (Belczynski et al. 2014).

To estimate the RLOF mass transfer rate $\dot{M}_{\rm RLOF}$ we evaluate donor properties and various angular momentum loss mechanisms in a given binary as described in Belczynski et al. (2008a). It is highly uncertain how the RLOF mass transfer rate is to be converted to X-ray luminosity, and we discuss this issue below.

The gravitational energy of the RLOFing material becomes converted into radiation in an accretion disk formed around the compact object (Shakura & Sunyaev 1973 see Lasota 2015 for a recent review on accretion disk physics). There are a number of effects that have a pivotal influence on the $\dot{M}_{\rm RLOF}$ to $L_{\rm X}$ conversion process in high mass accretion rate disks (see Figure 1).

The first conundrum to consider is the role of winds launched from the disk surface. Such winds have been ubiquitously detected in high mass accretion rate disk-dominated states of XRBs (e.g., Ponti et al. 2012, 2015). Winds are able to remove a substantial fraction of matter that is being transferred through the disk toward the compact object. At the same time, winds carry away the angular momentum and therefore influence the orbital evolution. We introduce the quantity $f_{\rm acc}$ to describe the fraction of $\dot{M}_{\rm RLOF}$ that is not affected by the disk winds ($\dot{M}_{\rm acc}$).

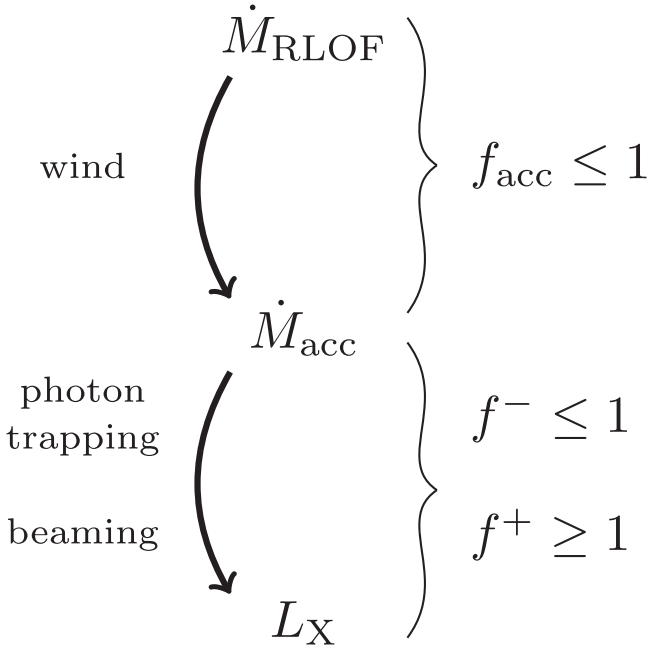

Figure 1. Most important processes behind conversion of RLOF mass transfer rate $\dot{M}_{\rm RLOF}$ into X-ray luminosity. Our parametrization of these processes is discussed in detail in Section 2 and used in Equation (1).

Second, not all of the photons produced in the vicinity of the accretor get emitted from the disk. Some of them are dragged by the inflowing matter and fall onto the compact object. As a result of this "photon trapping" effect (e.g., Ohsuga 2007a, hereafter O07; Abramowicz & Straub 2008; Narayan et al. 2012; Sądowski et al. 2015, hereafter S15), the observed X-ray luminosity is reduced. To include this and other currently unknown processes that may lower $L_{\rm X}$ we introduced the f^- parameter.

Finally, we took into account the processes that may increase the observed $L_{\rm X}$ due to non-isotropic emission. We utilize the f^+ factor, which, in addition to the beaming (King et al. 2001), may also include a contribution due to disk geometry, BH spin, column accretion in magnetized NS, etc. The beamed emission will always exceed the isotropic one ($f^+ > 1$; as an example, if the emission goes into a cone of opening angle 1°, 10° or 100°, it will correspond to $f^+ \sim 2.6 \times 10^4$, $\sim$260, and $\sim$2.8, respectively). However, a beamed source will be visible only from the directions enclosed by the cone, and thus its detection probability will be lower than that of an isotropic emitter.

The XRB X-ray luminosity is calculated as

$$L_{\rm X} = f^- f^+ \frac{\epsilon G M_{\rm acc}\, f_{\rm acc}\, \dot{M}_{\rm RLOF}}{R_{\rm acc}} = \eta \dot{M}_{\rm RLOF} c^2, \qquad (1)$$

where the radius of the accretor, $R_{\rm acc}$, is 10 km for a NS and 3 Schwarzschild radii for a BH, ϵ gives a conversion efficiency of gravitational binding energy to radiation associated with accretion onto a NS (surface accretion $\epsilon = 1.0$) and onto a BH (disk accretion $\epsilon = 0.5$), $\eta = f^- f^+ f_{\rm acc}\, \eta_0$ is the total efficiency of the accretion flow, and η_0 is the radiative efficiency of a standard thin disk.[6]

In our simulations we define a potential EULX source as the one with $L_{\rm X} > 10^{42}$ erg s^{-1}.

[5] http://boinc.berkeley.edu/

[6] In our case $\eta_{0,\rm BH} = 1/12$ and $\eta_{0,\rm NS} \approx 0.2$ (e.g., Shakura & Sunyaev 1973).

2.1. The Reference Model

In our reference model we assume no winds ($f_{\rm acc} = 1$), no photon trapping ($f^- = 1$), no beaming ($f^+ = 1$), and always efficient mass accretion rate-into-luminosity conversion (η_0 as in the standard thin disk). We adopt this condition even for very high RLOF mass transfer rates. This is quite arbitrary, however, our goal was to estimate the highest luminosities potentially reachable by an X-ray binary system without invoking strong beaming. On the other hand, $\eta = \eta_0$ may also correspond to a situation when a significant part of the $\dot{M}_{\rm RLOF}$ is lost from the system ($f_{\rm acc} < 1$) or $L_{\rm X}$ is lowered due to photon trapping ($f^- < 1$) but the beaming compensates these effects ($f^+ = 1/f_{\rm acc}f^-$). Numerical simulations (e.g., S15) suggest that $f_{\rm acc}$ is indeed small. However, f^+ may reach 10^3–10^4 for the cone opening angles on the order of a few degrees.

Therefore, with our reference model we obtain the maximum potential X-ray luminosity of a given binary system if the non-standard accretion disk effects are negligible or compensate each other.

2.2. The Ohsuga Model

Next, we have considered a BH accretion case with $\dot{M}_{\rm acc} < \dot{M}_{\rm RLOF}$ ($f_{\rm acc} < 1$), and $\dot{M}_{\rm acc}$ constrained following the results of O07 who performed global, axisymmetric simulations of supercritical disks with the αP viscosity, including effects of outflowing winds and photon trapping. We use the parametrization of the O07 results ($\dot{M}_{\rm acc}$ as a function of $\dot{M}_{\rm RLOF}$) derived in Belczynski et al. (2008b),

$$\log\left(\frac{\dot{M}_{\rm acc}}{\dot{M}_{\rm crit}}\right) = 0.934\log\left(\frac{|\dot{M}_{\rm RLOF}|}{\dot{M}_{\rm crit}}\right) - 0.380. \quad (2)$$

where $\dot{M}_{\rm crit} = 2.6 \times 10^{-8}(M_{\rm BH}/10\,M_\odot)\,M_\odot\ {\rm yr}^{-1}$ is the critical mass accretion rate. To obtain X-ray luminosities we utilized the Equation (1) using $\dot{M}_{\rm acc}$ as provided by Equation (2) and substituting $f^-f^+f_{\rm acc}\dot{M}_{\rm RLOF} = \dot{M}_{\rm acc}$. For a $10\,M_\odot$ BH accretor we obtain 2.8 times lower luminosity if $\dot{M}_{\rm RLOF} = 10^{-7}\dot{M}$ yr^{-1} and 6.7 times lower if $\dot{M}_{\rm RLOF} = 0.1\dot{M}$ yr^{-1}. For illustration, if the collimation angle of the outflow is $\sim 20°$, as in NS simulations of Ohsuga (2007b), the corresponding f^+ will be equal 66. The accretion onto NSs is limited to the classical Eddington limit in this model (Ohsuga 2007b). $L_{\rm X}$ is calculated as in Equation (1). We note that we have extrapolated results of the original calculations of Ohsuga (2007a) to the range of mass transfer rates we have in our simulations.

2.3. The Sądowski Model

Finally, we have experimented with the constraints on the $\dot{M}_{\rm acc}$ and $L_{\rm x}$ following the recent results of S15. The accretion rate at the BH horizon was found to be only a fraction of the RLOF rate,

$$\dot{M}_{\rm acc} = \dot{M}_{\rm RLOF}\frac{R_{\rm in}}{R_{\rm out}}, \quad (3)$$

where $R_{\rm out}$ and $R_{\rm in} = 20R_{\rm g}$ (Sądowski et al. 2014) are the outer and inner radii of the wind emitting region, respectively. It is hard to estimate the location of the outer edge, so we assumed a constant fraction $R_{\rm wind}/R_{\rm out} = 0.01$ (the wind probably is not emitted out to the edge of the disk), which corresponds to $f_{\rm acc} = 0.01$. In this model we utilized a different formula for X-ray luminosity which already accounts for the effects of photon trapping and beaming,

$$L_{\rm X} = 4 \times 10^{38} \times e^{-\frac{\theta}{0.2}}\frac{\dot{M}_{\rm acc}}{\dot{M}_{\rm Edd}}\frac{M_{\rm BH}}{M_\odot}\ {\rm erg\ s}^{-1}, \quad (4)$$

where θ is the viewing angle, $\dot{M}_{\rm Edd} = 2.44 \times 10^{18}\frac{M}{M_\odot}$ g s^{-1} is the Eddington accretion rate. In our simulations we incorporated θ in the range 0°–30° (the opening angle is 60°). This will correspond to $f^+ \approx 8$ in our reference model. In Sądowski et al. (2015) model we get different luminosities for different viewing angles, which was included in our simulations to calculate probabilities of observing a particular system as the EULX. Even though the S15 model was constructed for systems with BHs, we assumed that the same prescription is valid for the NSs accretors. We note that the results of O07 can be put in the framework of this model by taking $R_{\rm out} \approx 50R_{\rm g}$, which is approximately the effective circularization radius (and the outer edge of the disk) of the gas injected into their simulation box. We note that the Equation (4) was obtained by Sądowski et al. (2015) for supermassive BH, but we extrapolated it to the stellar mass ones.

3. RESULTS

Under the least restricting assumption (no limit on accretion rate, $\eta = \eta_0$) our EULX rate/number estimates are to be considered upper limits. We find that 1 per 44 billion binaries could potentially be an EULX with a BH accretor, and 1 per 44 billion binaries could potentially be an EULX with an NS accretor. This estimate employs a canonical IMF (Kroupa & Weidner 2003).

Figure 2 shows our upper limits for the number of EULXs with BH and NS accretors. Note that in our reference model we obtain virtually as many potential EULXs with a NS as with a BH accretor. This estimate accounts for the specific lifetime of each binary in a potential EULX phase. We assumed that the typical density of Milky Way equivalent galaxies (MWEG) in the local universe is $\rho_{\rm MWEG} = 0.01\,{\rm Mpc}^{-3}$. Currently, the observations place the only confirmed EULX (HLX-1) at the distance of 95 Mpc (Wiersema et al. 2010, but see Lasota et al. 2015). Our predicted upper limit on the number of EULXs at this distance is 90 and 93 binaries with BH and NS accretors, respectively. Both estimates significantly exceed the observed number of sources.

Had we imposed the classical Eddington limit on the mass accretion rate in our reference model, the number of EULXs would be zero for both types of accretors.

Table 1 introduces typical companion stars of our EULXs. Majority of the NS EULXs (92%) are found in binaries with helium star donors: either a $\sim 1.2\ M_\odot$ helium Hertzsprung gap star (HeHG) or a $\sim 1.8\ M_\odot$ helium Giant Branch (HeGB) star. The BH EULXs predominantly contain a hydrogen-rich stars that have just evolved beyond main sequence. Typically, these are $\sim 6\ M_\odot$ Hertzsprung gap (HG) stars (92.4%). The mass distributions of these most common EULX companions are presented in Figure 3. Table 2 contains typical evolutionary routes that lead to the formation of EULXs.

As a result of implementing the slim disk model of O07, the X-ray luminosities of our systems drop by a factor of at least

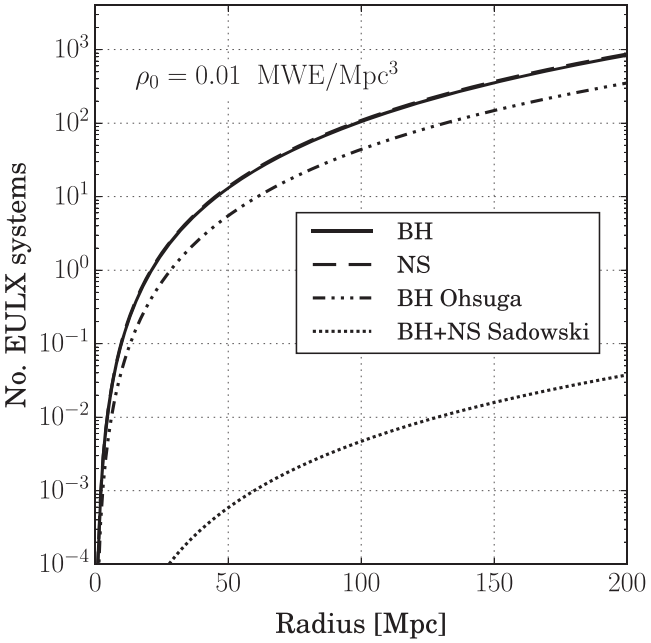

Figure 2. Upper limits on the number of EULXs within the sphere of radius R (solid for BH systems, dashed for NS systems) obtained under the assumption that a compact object can accrete at an arbitrary high rate (our reference model, Section 2.1). Note that had we imposed the classical Eddington limit in our reference model, the predicted number of extreme ULXs would be zero. The dot–dashed and dotted lines correspond to the limited accretion scenarios, with L_X calculated from the following models of O07 and S15 respectively.

2.8. Nevertheless, in this framework it is still possible to significantly exceed the classical Eddington limit. The estimated number of the BH EULX systems decreases to 1 in 105 billion binaries, and the number of BH EULXs within 100 Mpc is 37 (Figure 2).

After employing the model of S15 the upper limit on a number of expected EULXs drops to 1 per 2×10^{15} binaries. The expected upper limit on the number of EULX systems in the distance range of HLX-1 is 0.004. This is several orders of magnitude lower than in the two other models we tested.

In all cases, the EULX luminosities are achieved during the thermal timescale RLOF. The thermal RLOF mass transfer rate is calculated following Kalogera & Webbink (1996) as

$$\dot{M}_{\rm RLOF,th} = \frac{M_{\rm don}}{\tau_{\rm th}} = \frac{1}{3} \times 10^{-7} \frac{R_{\rm don} L_{\rm don}}{M_{\rm don}} M_\odot \ {\rm yr}^{-1}, \qquad (5)$$

where donor mass, radius, and luminosity are expressed in solar units. For example an EULX with a BH can start with a $\sim 10\,M_\odot$ HG donor, that has $\sim 20\,R_\odot$ radius and luminosity of $\sim 2 \times 10^4 L_\odot$. The donors in NS systems are evolved (post core He burning) low-mass helium stars that on the onset of RLOF have mass $\sim 2\,M_\odot$, radius $\sim 30\,R_\odot$ and luminosity $\sim 2 \times 10^4 L_\odot$. These parameters allow for very high RLOF mass transfer rates ($\dot{M}_{\rm RLOF,th} \sim 10^{-2}$–$10^{-3}\,M_\odot\ {\rm yr}^{-1}$. If this mass transfer is efficiently converted to X-ray luminosity ($\eta = \eta_0$), it will correspond to $L_{\rm x} \gtrsim 10^{42}$–$10^{43}$ erg s^{-1}) alas on a very short timescale ($\tau_{\rm th} \sim 10^2$–10^4 years).

Typical evolutionary routes that lead to the formation of a potential BH and NS EULX when $\eta = \eta_0$ are detailed in Sections 3.1–3.2. The corresponding time behavior of the mass accretion rate and maximum X-ray luminosity are shown in Figures 4 and 5.

3.1. BH EULX

A typical BH EULX system evolves along the evolutionary route BH/1 presented in Table 2. Its evolution begins with a $33\,M_\odot$ primary and $11\,M_\odot$ secondary on an orbit with separation $\sim 5500\,R_\odot$ and eccentricity $e = 0.56$. In 5.5 Myr the primary starts crossing the HG. At that point the orbit has expanded to $5900\,R_\odot$ due to wind mass loss from the primary (now $30\,M_\odot$). After about 10,000 years and significant radial expansion ($1300\,R_\odot$), the primary begins core helium burning (CHeB). As the primary approaches its Roche lobe tidal interactions circularise the orbit. After some additional expansion (radius $1700\,R_\odot$) and mass loss the primary ($18\,M_\odot$) initiates a common envelope (CE) phase. Following the envelope ejection the orbit contracts to $40\,R_\odot$ and the primary becomes a Wolf–Rayet star with the mass of $11\,M_\odot$. After 6.2 Myr of evolution the primary undergoes a core collapse and forms a $7.2\,M_\odot$ BH. At this time the orbit is rather compact ($a = 47\,R_\odot$) and almost circular ($e = 0.04$).

After the next 13 Myr the secondary enters the HG with a mass of $11\,M_\odot$ and radius $10\,R_\odot$, and expands filling its Roche lobe ($R_{\rm lobe} = 19\,R_\odot$). The mass transfer begins at orbital separation of $46\,R_\odot$. The luminosity of the donor is 21,000 $L_\odot$. Initially, for a short period of time (6000 years) the mass transfer proceeds on the donor thermal timescale with the RLOF mass transfer rate of $\dot{M}_{\rm RLOF} = 1.2 \times 10^{-3}\,M_\odot\ {\rm yr}^{-1}$ (corresponding to $L_{\rm x} = 5.8 \times 10^{42}$ erg s^{-1}). We allow the entire transferred material to accrete onto the BH. After mass ratio reversal, the orbit begins to expand in response to the mass transfer and the RLOF slows down. However, for the next 2000 years the donor RLOF rate stays above $2.2 \times 10^{-4}\,M_\odot\ {\rm yr}^{-1}$ ($L_{\rm x} = 10^{42}$ erg s^{-1}) and the system is still classified as a potential EULX. The evolution of the mass transfer rate throughout the RLOF phase is shown in Figure 4.

The RLOF terminates when the secondary has transferred most of its H-rich envelope to the BH (with the final mass $14\,M_\odot$). The reminder of the secondary envelope is lost in a stellar wind and the secondary becomes a naked helium star with the mass of $2.5\,M_\odot$. At this point the binary separation is $230\,R_\odot$. The low-mass helium secondary ends its evolution in the SN Ib/c explosion forming a low-mass NS ($\sim 1.1\,M_\odot$). The natal kick (if significant) is very likely to disrupt the system.

3.2. NS EULX

A typical system (NS/1 channel in Table 2) begins as a $10\,M_\odot$ primary and a $5.6\,M_\odot$ secondary on a $700\,R_\odot$ orbit with an eccentricity $e = 0.73$. In 24 Myr the primary enters the HG. After 50,000 years of expansion on the HG the primary overfills its Roche lobe at the radius of $85\,R_\odot$. The orbit circularises and becomes $190\,R_\odot$. We assume a non-conservative mass transfer in such a case, and allow 50% of transferred material to accumulate on the main sequence secondary. At the end of this RLOF episode the primary becomes a low-mass helium star ($2.2\,M_\odot$) and the secondary becomes a rejuvenated main sequence star ($9.5\,M_\odot$). The separation has expanded to $640\,R_\odot$. The low-mass helium star evolves and expands after its core He burning is completed. When the radius of the primary ($200\,R_\odot$) exceeds its Roche lobe, the second phase of a non-conservative mass transfer is initiated. At this point the separation is $720\,R_\odot$ and the masses are $2.06\,M_\odot$ and 9.45 for the primary and secondary, respectively. After a short phase of a RLOF (4000 years) and after 28.6 Myr since the zero age main

Table 1
Compact Accretors and their Typical Companions

Accretor Type[a]	Companion Type[b]						
NS EULX	RG	EAGB	**HeHG**	**HeGB**	CO WD	ONe WD	
2.6×10^{-3}/MWEG	6.35%	6.4×10^{-3}%	**48%**	**44%**	0.5%	0.8%	
BH EULX	MS	**HG**	RG	CHeB	EAGB	HeHG	HeGB
2.5×10^{-3}/MWEG	3.4%	**92.4%**	1%	0.3%	0.5%	0.5%	0.3%

Notes.
[a] Type of accretor and the number of EULXs in the Milky Way Equivalent galaxy.
[b] Percentage of EULX systems with the same type of accretor, MS—Main Sequence, HG—Hertzsprung Gap, RG—Red Giant, CHeB—Core Helium Burning, EAGB—Early Asymptotic Giant Branch, **HeHG**—Helium Hertzsprung gap, HeGB—Helium Giant Branch, CO WD—Carbon–Oxygen White Dwarf, ONe WD—Oxygen–Neon White Dwarf. Mass distributions of bolded configurations are presented in Figure 3.

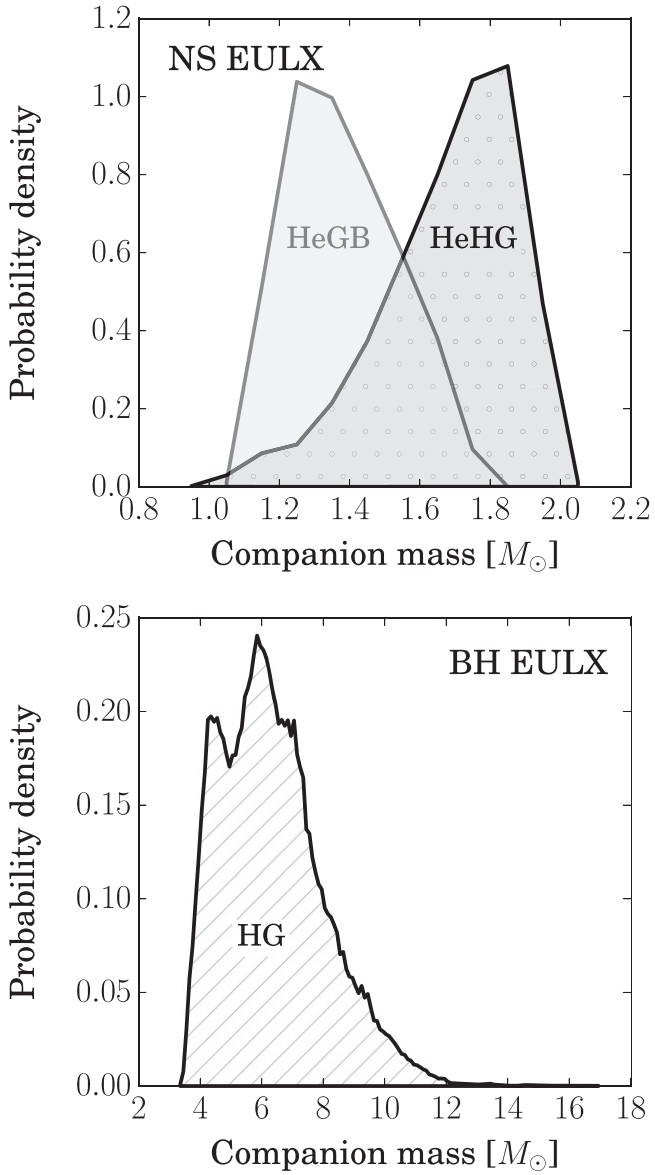

Figure 3. Mass distribution of the most common companions in NS (top) and BH (bottom) systems during the EULX phase in our reference model (Section 2.1). In the BH systems nearly all companions are on the Hertzsprung Gap (HG) with masses in the 4–10 $M_\odot$ range, while the NS companions typically enter the EULX phase as helium Hertzsprung Gap (HeHG) stars and evolve to helium Giant Branch stars (HeGB).

sequence (ZAMS), the primary explodes in electron capture supernova and forms a low-mass NS (1.26 $M_\odot$). We assume zero natal kick in this case and the system survives the explosion.

After additional 20 Myr the 9.3 $M_\odot$ secondary leaves the main sequence and evolves through the HG to become a red giant. Expansion on the red giant branch leads to a RLOF that due to a large mass ratio and a deep convective envelope of the secondary turns into a CE phase. At the onset of the CE, the separation is 600 $R_\odot$ and the secondary radius is 330 $R_\odot$. We assume energy balance for the CE (Webbink 1984), and obtain the post-CE separation of 50 $R_\odot$. The secondary has lost its entire H-rich envelope and becomes a low-mass helium star (2 $M_\odot$). After CHeB, the low-mass secondary begins to expand and finally overfills its Roche lobe at the radius of 27 $R_\odot$ (the corresponding binary separation is 55 $R_\odot$). At this point the evolved helium star crosses the HeHG and drives a high rate mass transfer ($\dot{M}_{\rm RLOF} = 7.8 \times 10^3\, M_\odot\ {\rm yr}^{-1}$; $L_{\rm X} = 8 \times 10^{43}$ erg s^{-1}) onto its NS companion. Since in our first approximation we have assumed a fully efficient accretion with no limit, the NS mass quickly increases to 2 $M_\odot$. The RLOF phase is very short (100 years), and it drives an extremely high mass transfer rate allowing this system to become a potential EULX with a NS accretor (see Figure 5). Finally, the secondary is depleted of its He-rich envelope and forms a naked CO core that cools off to become a CO WD. After 51.6 Myr since the ZAMS we note the formation of a wide NS-WD binary (separation of 60 $R_\odot$), with the gravitational merger time exceeding the Hubble time ($t_{\rm merger} = 2.8 \times 10^{14}$ years).

4. DISCUSSION

By allowing that all matter transferred through the RLOF is accreted ($\dot{M}_{\rm acc} = \dot{M}_{\rm RLOF}$) and converted efficiently into X-rays ($L_{\rm X} = \eta \dot{M}_{\rm acc} c^2$, where $\eta = \eta_0$ as in the standard disk), we are able to form a large number of potential BH *and* NS EULX systems. The EULX phases that we obtain are short (~10,000 years and ~100 years for BH and NS systems, respectively). Nevertheless, we observe them in 0.1% of all simulated binaries. Our parameter space covers all progenitors of XRBs, so every 1 in 1000 XRBs should become an EULX during its evolution. Luminosities that we find in our simulations exceed 10^{42} erg s^{-1}. Such high luminosities are found both for BH and NS accretors. Particularly, the presence of the potential EULXs with NS accretors in our results seems to agree with the recent discovery of the NS ULX system M82 X-2 (Bachetti et al. 2014).

Evolution of ULXs with NS accretors was also the topic of a recent work by Fragos et al. (2015). They used the BSE code

Table 2
Typical EULX Evolutionary Routes

Accretor/Route	%[a]	Number/MWEG[b]	Evolutionary Route[c]
NS/1	50%	1.3×10^{-3}	MT1(2/3-1) MT1(8/9-1) SN1 CE2(13-3/4;13-7) MT2(13-8/9)
NS/2	40%	1.0×10^{-3}	MT1(2/3-1) SN1 CE2(13-3/4;13-7) MT2(13-8/9)
NS/3	10%	2.6×10^{-4}	Other
BH/1	97%	2.5×10^{-3}	CE1(4–1;7–1) SN1 MT2(14–1/2/3/4/5)
BH/2	3%	6.8×10^{-5}	Other

Notes.
[a] Percentage of the systems with the same type of accretor.
[b] Number of systems expected to be observed per Milky Way Equivalent galaxy.
[c] Symbolic designation of the evolutionary routes; MT1/MT2—mass transfer from the primary/secondary, SN1—supernova explosion. CE1/CE2—common envelope phase started by the primary/secondary. Numbers inside the parentheses specify the evolutionary phases of the stars: 1-MS; 2-HG; 3-RG; 4-CHeB; 5-EAGB; 7-HeMS; 8-HeHG; 9-HeGB; 13-NS; 14-BH (see Belczynski et al. 2008a for details).

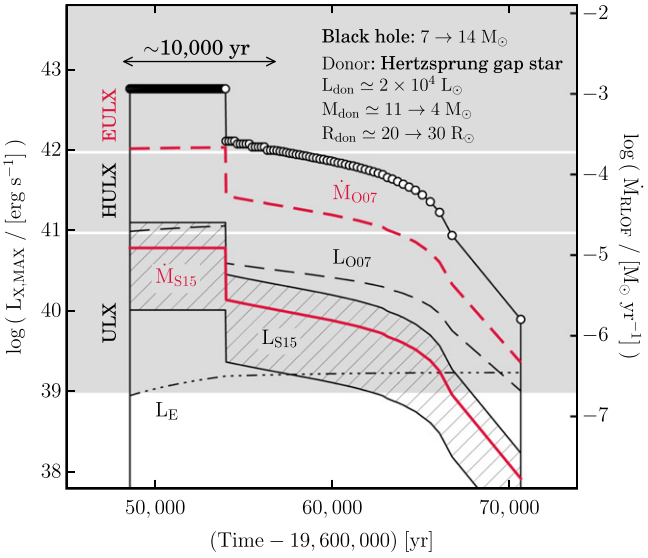

Figure 4. Typical evolution through Roche lobe overflow for a potential BH EULX binary in our reference model (open circles, $\eta = \eta_0$, see Section 2.1). A 11 $M_\odot$ Hertzsprung gap star transfers its H-rich envelope to a 7 $M_\odot$ black hole. The mass transfer during the EULX phase is driven on a thermal timescale of the donor (~10,000 years) at a very high rate $\sim 10^{-3}\, M_\odot\ \mathrm{yr}^{-1}$ (see Section 3.1). The thick/red solid line and the hatched area represent, respectively, the mass accretion rate and the range of viewing angle dependent luminosities ($\theta = 0°$–$30°$) obtained for our $\dot{M}_{\rm RLOF}$ time evolution with the model of S15 ($f_{\rm acc} = 0.01$, $f^+ = 8$). Similarly, the thick/red dashed line and thin/black dashed line show the mass accretion rate and luminosity derived with the model of O07 ($f_{\rm acc} \simeq 0.2$–0.3, $f^+ \approx 66$). The classical Eddington limit is marked with dot–dashed line.

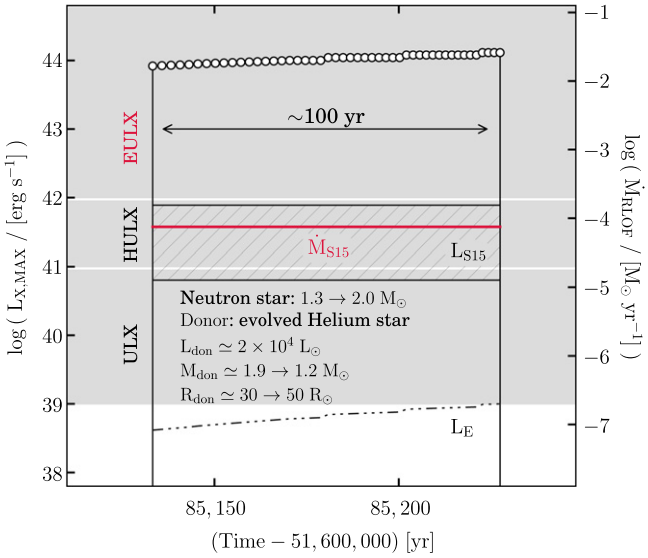

Figure 5. Typical evolution through Roche lobe overflow for a potential NS EULX binary system in our reference model (open circles, $\eta = \eta_0$, see Section 2.2). A 1.9 $M_\odot$ evolved helium star transfers its He-rich envelope to a neutron star. The mass transfer is driven on a very short thermal timescale (~100 years) at a rate $\sim 10^{-2}\, M_\odot\ \mathrm{yr}^{-1}$ (see Section 3.2). The thick/red solid line and the hatched area represent, respectively, the mass accretion rate and range of viewing angle dependent luminosities obtained for our $\dot{M}_{\rm RLOF}$ evolution with the model of S15 ($f_{\rm acc} = 0.01$, $f^+ \approx 8$). Note that the model of S15 considers the case of BH accretion, however, in the case of a NS accretor, we assumed the same prescription for L_X.

for evolution of binaries and the MESA code to calculate precisely the mass transfer phases. They found that NS ULX systems should exist in 13% of M82-like galaxies. They also found donors to be H-rich stars with masses in the 3–8 $M_\odot$ range and 1–3 day orbital periods. The orbits in our NS EULX systems are wider (~30 days periods) and the companion stars are lighter (1–2 $M_\odot$) and of a different type (evolved helium stars) than those reported in Fragos et al. (2015). They obtained mass transfer rates up to $\dot{M}_{\rm RLOF} \approx 10^{-2}\, M_\odot\ \mathrm{yr}^{-1}$ (see their Figure 4), so they have reached mass transfer rates approximately as high as in our study. However, it needs to be noted that they have studied a much broader population of ULXs, while we have focused only on the brightest ones.

A problem of the maximum X-ray luminosity available from a binary system was considered also by Podsiadlowski et al. (2003). However, their study was confined to only 11 evolutionary routes, only BH binary systems, and quite limited parameter space (systems composed initially of a primary with mass in the 25–45 $M_\odot$ range and a 2–17 $M_\odot$ secondary mass range). Rappaport et al. (2005) extended the simulations of Podsiadlowski et al. (2003) and were able to obtained ULXs with X-ray luminosities of 3×10^{42} erg s^{-1} (see their Figure 11) for a 5 $M_\odot$ BH and 9 $M_\odot$ donor and the case B mass transfer (HG donor). This is consistent with our typical BH EULX system. Their secondaries also fill their Roche lobe due to expansion of the envelope, and the ULX phase lasts at most a few Myr (about 10,000 years as EULX). However, their grid of parameters is far more sparse than ours, as they simulated

only 52 specific evolutionary cases in comparison to our 10^9 evolutionary routes.

Podsiadlowski et al. (2003) and Rappaport et al. (2005) used a detailed evolutionary code to obtained their results, while we used a simplified evolutionary formulae to cover larger parameter space. Both approaches have their advantages. With our approach we could not only confirm, but also extend the previously published results, both in terms of the accretor type (NS accretors possible) and in the range of potentially available mass transfer rates onto compact accretors in close binary systems.

Reference model scenarios lead to a significant overestimate of the number of the potential EULX systems in the local universe. We find close to ∼100 systems with an NS, and a similar number of systems with a BH within the 100 Mpc radius. Note that these numbers should be considered as upper limits. However, to date observations have revealed only one system with $L_X > 10^{42}$ erg s^{-1}, HLX-1 (Farrell et al. 2011).

Observational data indicates that HLX-1 is a transient system with recurrent outbursts on timescales of about 1 year (e.g., Godet et al. 2009). Thermal-viscous instability mechanism was proposed to drive outburst in XRBs. However, this mechanism is not operational for mass transfer rates exceeding $(a\ few) \times 10^{-5}\,M_\odot$ yr^{-1} because the disk becomes too hot and thus constantly ionized (Lasota et al. 2015). If the periodicity observed in HLX-1 is connected to thermal-viscous instability, then the mass transfer rate needs to be lower than the above threshold, and high X-ray luminosity is achieved by effective beaming of radiation.

Since our reference model provides only a very crude estimate of X-ray luminosity, we proceeded with investigating the state-of-the-art global accretion models of the super-Eddington accretion regime. O07 performed 2D radiation hydrodynamic simulations of supercritical accretion disks around BHs with the αP viscosity, while S15 performed simulations of the magnetized accretion disks in general relativity using radiation MHD code KORAL. The former simulations were fed by inflowing stream of gas circularizing near $R_{\rm cir} = 100R_{\rm G}$, while the latter were initialized as equilibrium torii threaded by seed magnetic field. Both models agree that there is significant mass loss in the accretion flow, driven either by radiation pressure itself, or by radiation pressure and the centrifugal force. The work by O07 provides a dependence of the mass accretion rate and luminosity on the mass input rate (here $\dot{M}_{\rm RLOF}$). However, this result depends strongly on the assumed location of the circularization radius, i.e., it implicitly assumes that no gas is lost outside $R \approx 100R_{\rm G}$. In real RLOF systems, the outer edge of the disk is expected to be located much farther (up to about 2/3 Roche lobe radius of the accretor). The other approach S15 was not limited by the disk truncation inside the simulation box, but rather by the computational time, which allowed flow to reach the inflow/outflow equilibrium only to radius $R_{\rm eq} \approx 100R_{\rm G}$. Inside this region, the gas flows out as wind down to $R_{\rm wind} \approx 20R_{\rm G}$, and shows a roughly constant mass loss rate $d\dot{M}_{\rm wind}/dR$. The total amount of gas lost in the system will therefore depend on the location of the outer disk edge, or rather the outer edge of the wind emitting region, through Equation (3). Because of poor understanding of the dynamics in the outer region of accretion disks, we assumed $R_{\rm wind}/R_{\rm out} = 0.01$.

Within all of the discussed-here accretion models, binary systems are able to breach the 10^{42} erg s^{-1} EULX limit. Although, in the case of S15 the probability of forming a binary EULX is a few orders of magnitude smaller than for the other cases. Limitation of the mass accretion rate onto the BH in models developed in O07 and S15 results not only in lower X-ray luminosity, but also in different orbit evolution as compared to our typical EULX case presented in Figure 4. Both effects (lower X-ray luminosity and different orbit evolution) decrease the predicted number of EULXs in the local universe for O07 and S15 models.

If disk winds are effective, matter that cannot be accreted is ejected from the system and takes away angular momentum. As a result, the binary separation decreases and this prevents longer phases of high mass transfer. For the case of the O07 outflow model, the total time spent in the EULX regime is about 3000 years, as opposed to 10,000 years in our reference scenario. As a result, we estimated upper limit on the number of the potential BH EULXs drops in the O07 model from ∼100 to 37 within the 100 Mpc radius. In Figure 4 we show how the $\dot{M}_{\rm RLOF}$ of our typical BH EULX (the reference model) translates into L_X and $\dot{M}_{\rm acc}$ derived from the model of O07.

When we limit the $\dot{M}_{\rm acc}$ according to Equation (3) (S15), we find considerably fewer EULXs within the 100 Mpc radius than in the case of our reference model (a factor of $\sim 5 \times 10^4$ fewer). For the accretion limited case, in employing the model of O07 we obtain only a few times fewer number of EULXs (a factor of ∼3 fewer). Particularly, in the case of our typical BH EULX system (Figure 4) we find two orders of magnitude smaller luminosity in the beam than in the reference model. In Figure 4 we show the $\dot{M}_{\rm acc}$ and a range of $L_{\rm x}$ computed for $\theta = 0°$–$30°$ (Equations (3) and (4), respectively; Sądowski et al. 2015) corresponding to the mass transfer history $\dot{M}_{\rm RLOF}$ of our typical BH EULX (the reference model).

Both O07 and S15 considered accretion disks around BHs. The case of an NS accretion is far more complicated. A strong magnetic field associated with NSs may disrupt the disk far away from the accretor. Even if the magnetic field is weak, the emission will be weaker as the accretor mass is lower. On the other hand, the NS accretion efficiency (η) is higher than that of BHs as the matter and photons do not fall under the event horizon. To date, no comprehensive simulations of such a case have not been performed. Ohsuga (2007b) performed 2D simulations for a very limited range of initial parameters. They obtained supercritical accretion rates for NS accretors and provided information that the mass accretion rate is 20%–30% of that onto the BH for the same mass input rate. Thus, we have assumed NS Eddington limited accretion case in the Oshuga et al. models, but we have allowed super-Eddington accretion for Sądowski et al. models.

We note that had we imposed the logarithmic scaling of L_X with $\dot{M}_{\rm acc}$ (e.g., Poutanen et al. 2007), we would have not obtained any systems with luminosities in the EULX regime. There exist factors that can improve this situation, like beaming of the radiation, however, spherical nebulae observed around some of ULXs (Pakull & Mirioni 2002; Moon et al. 2011; Russell et al. 2011) may suggest dispersion of the outflow energy and nearly isotropic emission. The relation between $\dot{M}_{\rm acc}$ and L_X has not been derived from first principles, and advanced numerical models do not seem to confirm this relation (e.g., Ohsuga 2007a; Sądowski et al. 2015).

Gladstone et al. (2013) and Heida et al. (2014) presented programs to search for the companion stars of the ULX systems in the optical and infrared bands, respectively. The former group investigated close (∼5 Mpc) ULXs and discovered 13±5 optical

counterparts among 33 ULXs. The masses of the companions have large uncertainties and generally only the upper limit is provided in the mass range 5.7–16.1 $M_{\odot}$. In a few cases the lower limit is also present in the mass range 8.3–14.7 $M_{\odot}$. These constraints are in agreement with our results. Heida et al. (2014) investigated 62 close ULXs and discovered 17 potential counterpart candidates. Based on the absolute magnitudes most of them (11) are red supergiants. According to our results, the most common companions of the ULX systems able to reach the EULX regime are 6 $M_{\odot}$ Hertzsprung gap stars with BH accretors and 1–2 $M_{\odot}$ low-mass helium stars for NS accretors. However, it is possible that the red supergiants that we found to be in minority among the EULX companions are more typical in the case of standard ULX systems. Detailed investigation of the properties of the entire ULX population will be presented in our forthcoming paper.

5. CONCLUSIONS

We conducted a proof-of-concept study to investigate if a binary system can form a ULX with the extreme mass transfer rate potentially able to lead to the X-ray luminosities in the $>10^{42}$ erg s^{-1} range. This is at least hundred times more than what is expected for the Eddington limited stellar-origin 100 $M_{\odot}$ BH (Belczynski et al. 2010, 2014). Observations of HLX-1 in ESO 243-49 with X-ray luminosity of 1.1×10^{42} erg s^{-1} encouraged us to look into the problem.

We find several evolutionary channels that lead to phases of a very high mass transfer rate in close RLOF binaries. These evolutionary phases can be extremely short, but it appears that many binaries experience such phases. The mass transfer rate may so high that (if Eddington limit, or any similar limit is breached) the X-ray luminosity may reach well above 10^{42} erg s^{-1}. We have adopted two physical accretion disk models in XRBs, and we have shown that for each model (that takes into account mass loss from accretion flow and photon trapping) EULX sources are formed within typical stellar populations. We note that increasing the geometrical beaming of radiation, many more binaries than considered in our study could possibly become ULX or EULX.

It is found that about half of this potential extreme ULX systems host not BH, but NS accretors. This contradicts the present consensus in the community, as the brightest ULX systems are commonly suspected to host IMBH primaries. Or at the minimum with stellar-origin BHs.

We would like to thank volunteers whose participation in the universe@home test project[7] made it possible to acquire the results in such a short time. This study was partially supported by the Polish NCN grant N203 404939, Polish FNP professorial subsidy "Master2013," and by Polish NCN grant SONATA BIS 2 (DEC-2012/07/E/ST9/01360). M.S. was partially supported by the Polish NCN grant No. 2011/03/B/ST9/03459. K.B. also acknowledges NASA grant No. NNX09AV06A and NSF grant No. HRD 1242090 awarded to the Center for Gravitational Wave Astronomy, UTB.

REFERENCES

Abramowicz, M., & Straub, O. 2008, NewAR, 51, 73
Abt, H. A. 1983, ARA&A, 21, 343
Bachetti, M., Harrison, F. A., Walton, D. J., et al. 2014, Natur, 514, 202
Bachetti, M., Rana, V., Walton, D. J., et al. 2013, ApJ, 778, 163
Begelman, M. C., King, A. R., & Pringle, J. E. 2006, ApJ, 643, 1065
Belczynski, K., Bulik, T., Fryer, C. L., et al. 2010, ApJ, 714, 1217
Belczynski, K., Buonanno, A., Cantiello, M., et al. 2014, ApJ, 789, 120
Belczynski, K., Kalogera, V., Rasio, F. A., et al. 2008a, ApJS, 174, 223
Belczynski, K., Taam, R. E., Rantsiou, E., & van der Sluys, M. 2008b, ApJ, 682, 474
Colbert, E. J. M., & Mushotzky, R. F. 1999, ApJ, 519, 89
Crowther, P. A., Schnurr, O., Hirschi, R., et al. 2010, MNRAS, 408, 731
Dominik, M., Berti, E., O'Shaughnessy, R., et al. 2015, ApJ, 806, 263
Duquennoy, A., & Mayor, M. 1991, A&A, 248, 485
Fabbiano, G., Gioia, I. M., & Trinchieri, G. 1989, ApJ, 347, 127
Fabrika, S., Karpov, S., Abolmasov, P., & Sholukhova, O. 2006, in IAU Symp. 230, Populations of High Energy Sources in Galaxies, ed. E. J. A. Meurs & G. Fabbiano (Cambridge: Cambridge Univ. Press), 278
Farrell, S. A., Servillat, M., Wiersema, K., et al. 2011, AN, 332, 392
Fender, R., & Belloni, T. 2004, ARA&A, 42, 317
Fragos, T., Linden, T., Kalogera, V., & Sklias, P. 2015, ApJL, 802, L5
Gladstone, J. C., Copperwheat, C., Heinke, C. O., et al. 2013, ApJS, 206, 14
Godet, O., Barret, D., Webb, N. A., Farrell, S. A., & Gehrels, N. 2009, ApJL, 705, L109
Heida, M., Jonker, P. G., Torres, M. A. P., et al. 2014, MNRAS, 442, 1054
Kalogera, V., & Webbink, R. F. 1996, ApJ, 458, 301
King, A. R. 2008, MNRAS, 385, L113
King, A. R., Davies, M. B., Ward, M. J., Fabbiano, G., & Elvis, M. 2001, ApJL, 552, L109
Kluźniak, W., & Lasota, J.-P. 2015, MNRAS, 448, L43
Kobulnicky, H. A., Fryer, C. L., & Kiminki, D. C. 2006, ApJ, in press (arXiv: astro-ph/0605069)
Kroupa, P., Tout, C. A., & Gilmore, G. 1993, MNRAS, 262, 545
Kroupa, P., & Weidner, C. 2003, ApJ, 598, 1076
Lasota, J.-P. 2015, arXiv:1505.02172
Lasota, J.-P., King, A. R., & Dubus, G. 2015, ApJL, 801, L4
Liu, J. 2011, ApJS, 192, 10
Medvedev, A. S., & Poutanen, J. 2013, MNRAS, 431, 2690
Miller, M. C., & Hamilton, D. P. 2002, MNRAS, 330, 232
Moon, D.-S., Harrison, F. A., Cenko, S. B., & Shariff, J. A. 2011, ApJL, 731, L32
Motch, C., Pakull, M. W., Soria, R., Grisé, F., & Pietrzyński, G. 2014, Natur, 514, 198
Narayan, R., Sądowski, A., Penna, R. F., & Kulkarni, A. K. 2012, MNRAS, 426, 3241
Ohsuga, K. 2007a, ApJ, 659, 205
Ohsuga, K. 2007b, PASJ, 59, 1033
Pakull, M. W., & Mirioni, L. 2002, arXiv:astro-ph/0202488
Pasham, D. R., Strohmayer, T. E., & Mushotzky, R. F. 2014, Natur, 513, 74
Podsiadlowski, P., Rappaport, S., & Han, Z. 2003, MNRAS, 341, 385
Ponti, G., Bianchi, S., Muñoz-Darias, T., et al. 2015, MNRAS, 446, 1536
Ponti, G., Fender, R. P., Begelman, M. C., et al. 2012, MNRAS, 422, L11
Poutanen, J., Lipunova, G., Fabrika, S., Butkevich, A. G., & Abolmasov, P. 2007, MNRAS, 377, 1187
Rappaport, S. A., Podsiadlowski, P., & Pfahl, E. 2005, MNRAS, 356, 401
Russell, D. M., Yang, Y.-J., Gladstone, J. C., Wiersema, K., & Roberts, T. P. 2011, AN, 332, 371
Sądowski, A., Narayan, R., McKinney, J. C., & Tchekhovskoy, A. 2014, MNRAS, 439, 503
Sądowski, A., Narayan, R., Tchekhovskoy, A., et al. 2015, MNRAS, 447, 49
Servillat, M., Farrell, S. A., Lin, D., et al. 2011, ApJ, 743, 6
Shakura, N. I., & Sunyaev, R. A. 1973, A&A, 24, 337
Sutton, A. D., Roberts, T. P., Gladstone, J. C., & Walton, D. J. 2015, MNRAS, 450, 787
Sutton, A. D., Roberts, T. P., Walton, D. J., Gladstone, J. C., & Scott, A. E. 2012, MNRAS, 423, 1154
Villante, F. L., Serenelli, A. M., Delahaye, F., & Pinsonneault, M. H. 2014, ApJ, 787, 13
Walton, D. J., Fuerst, F., Harrison, F., et al. 2013, ApJ, 779, 148
Walton, D. J., Roberts, T. P., Mateos, S., & Heard, V. 2011, MNRAS, 416, 1844
Webbink, R. F. 1984, ApJ, 277, 355
Wiersema, K., Farrell, S. A., Webb, N. A., et al. 2010, ApJL, 721, L102
Yusof, N., Hirschi, R., Meynet, G., et al. 2013, MNRAS, 433, 1114

[7] http://universeathometest.info